Isoform-dependent interaction of voltage-gated sodium channels with protons

A. Khan, J. W. Kyle, D. A. Hanck, G. M. Lipkind and H. A. Fozzard

The Cardiac Electrophysiology Laboratories, Departments of Medicine and of Biochemistry and Molecular Biology, The University of Chicago, Chicago, IL 60637, USA

Protons are potent physiological modifiers of voltage-gated Na^+ channels, shifting the voltage range of channel gating and reducing current magnitude ($pK_a \sim 6$). We recently showed that proton block of the skeletal muscle isoform ($Na_V1.4$) resulted from protonation of the four superficial carboxylates in the outer vestibule of the channel. We concluded that the large local negative electrostatic field shifted the outer vestibule carboxylate pK_a into the physiological range. However, block was not complete; the best-fit titration curves yielded an acid pH asymptote of 10–15%, suggesting that the selectivity filter carboxylates may not be protonated. Using HEK 293 cells stably expressing different isoforms, each with varying channel density, we demonstrate that a pH-independent current is found in $Na_V1.4$, but not in the cardiac isoform ($Na_V1.5$). Mutational studies showed that absence of the pH-independent current in $Na_V1.5$ could be ascribed to the cysteine in domain I, just above the selectivity filter aspartate (Cys373). We suggest that this cysteine can be protonated in acid solution to produce a positive charge that blocks the pore. Competition between protons and Na^+ did not exist for Na^+ concentrations between 1 and 140 mM. The residual current in acid solution, when the cysteine is absent, confirms that over the range of pH values that can be achieved physiologically, the selectivity filter carboxylates are not protonated. The pH-independent current helps to protect activation of skeletal muscle during the acidosis that occurs during exercise.

(Received 20 June 2006; accepted after revision 26 July 2006; first published online 27 July 2006)
Corresponding author H. A. Fozzard: PO Box 574, 16 Georgianna Lane, Dana, NC 28724, USA.
Email: hafozzar@uchicago.edu

The highly charged Na^+ channel outer vestibule includes an outer ring of four carboxylates, and an inner selectivity ring with two carboxylates (Asp and Glu), and a lysine – the 'DEKA motif' (Terlau *et al.* 1991). All of these carboxylates are known to contribute to permeation because mutation of each individually to neutral residues reduces single-channel conductance (Terlau *et al.* 1991; Chiamvimonvat *et al.* 1996*a*,*b*). We recently demonstrated in an oocyte expression system that reduction of Na^+ channel current (I_{Na}) in acid solutions results from protonation of the four outer vestibule carboxylates (Khan *et al.* 2002). How the deprotonated carboxylates contribute to permeation is not clear. For voltage-dependent K^+ channels (Nimigean *et al.* 2003), charges at the entrance to the inner pore produce a local electrostatic field that probably concentrates K^+ on one side of the selectivity filter, resulting in asymmetrical effects on inward and outward currents. This mechanism is unlikely to apply to the Na^+ channel because its conductance–voltage relationship in symmetrical Na^+ is nearly linear in the physiological range (e.g. Green *et al.* 1987; Schild & Moczydlowski, 1994; Schlief *et al.* 1996), and reduced conductance from mutational neutralization cannot be overcome by saturating Na^+ concentrations (Chiamvimonvat *et al.* 1996*b*).

We suggested that the outer ring and selectivity filter carboxylates may all cooperate in ion permeation, but that the two selectivity ring carboxylates are protected from protonation in acid solution by the positive electrostatic field of the adjacent lysine residues (Khan *et al.* 2002). Supporting this idea was suggestion of a pH-independent current at acid pH (acid asymptote of the best-fit single-site titration curve was not zero), because protonation of the selectivity filter carboxylates would have reduced the current at low pH to near zero (Terlau *et al.* 1991; Chiamvimonvat *et al.* 1996*a*). However, we had few measurements in the very acid range because oocytes tolerate acid solutions poorly, so that effects often could not be reversed. We created stable cell lines in HEK 293 cells, a cell type that is more tolerant of acid solutions. In these cells, channel densities of varying magnitudes could be achieved so that the Na^+ concentration could be varied. A pH-independent current in $Na_V1.4$, the skeletal muscle isoform, was clearly seen, but it was

 DOI: 10.1113/jphysiol.2006.115659

surprisingly absent in $Na_V1.5$, the cardiac isoform, even though the vestibule carboxylates in these two isoforms are identical. Mutational analysis showed that loss of the pH-independent current was correlated with presence of cysteine just above the domain I selectivity aspartate in the vestibule P-loop (Cys373). We suggest that in acid solution the cysteine can be protonated, either creating an electrostatic barrier to permeation or neutralizing the adjacent selectivity filter aspartate. Consequently, in acid solution, the cardiac Na^+ current is completely blocked, but in muscle and nerve some current persists. This persistent current probably results from protection of the selectivity filter carboxylates from the outer vestibule negative field by the adjacent lysine common in all Na^+ channel isoforms. Acidosis commonly occurs locally in skeletal muscle during exercise. Although its role in fatigue is controversial (Westerblad & Allen, 2003), the pH-independent current seen in the $Na_V1.4$ channel and brain isoforms, which have a tyrosine or a phenylalanine in this position, would tend to protect muscle and nerve Na^+ channels from proton block.

Methods

Studies were made with the rat skeletal muscle Na^+ channel isoform, $Na_V1.4$ (μ1; originally given by J. R. Moorman, University of Virginia, Charlottesville, VA, USA), and the human cardiac sodium channel isoform, $Na_V1.5$ (hH1a; originally given by H. A. Hartmann, University of Maryland Biotechnology Institute, Baltimore, MD, USA). Methods used for producing mutations were as previously described (Khan *et al.* 2002; Sunami *et al.* 2004). For each channel studied here ($Na_V1.4$, $Na_V1.5$, $Na_V1.4$(Y401C), $Na_V1.5$(C373Y), $Na_V1.4$(Y401F) and $Na_V1.4$(Y401S)), stable cell lines were made in HEK 293 cells selected with 800 μg ml^{-1} G418 or 200 μg ml^{-1} Zeocin, or in HEK-Flp cells (Invitrogen, Carlsbad, CA, USA) selected with 200 μg ml^{-1} Zeocin. Cells were maintained in 100 mm Corning culture dishes containing Dulbecco's modified Eagle's medium (DMEM; Invitrogen) supplemented with 10% fetal bovine serum, penicillin (50 units ml^{-1}), streptomycin (50 μg ml^{-1}), and, for continued selection, 100 μg ml^{-1} Zeocin or G418.

For electrophysiology, cells were trypsinized (0.25% trypsin-EDTA; Invitrogen) from plates at 2–6 days after plating. Recordings were made with an Axopatch 200B amplifier, a Digidata 1322A digital/analog converter, and the pCLAMP 8.1 data acquisition software (Axon Instruments). Data were filtered at 10 kHz, and sampled at 100 kHz. All recordings were made at room temperature (20–22°C). Patch pipettes, constructed from microhaematocrit glass capillary tubes (Fisher), were typically filled with 10 mM NaCl, 130 mM CsF, 5 mM EGTA, and 10 mM Hepes titrated to pH 7.4 with CsOH. In some cases the NaCl in the pipette solution was increased to 20 mM, or reduced to 5.0, 1.0 or 0.5 mM, with compensatory changes in CsF in order to keep reversal potential of the current near 40 mV. The typical bath solution was 50 mM NaCl, 90 mM CsCl, 2 mM $CaCl_2$, and 10 mM Hepes titrated with CsOH to various pH values. Mes was substituted for Hepes for solutions having a pH value of <6.5. Various cell lines were used that expressed different current magnitudes, and the bath solution NaCl was increased to 140 mM or reduced to 10, 5, 2 or 1.0 mM, with compensatory changes in CsCl, as required. After each experiment, the pH of each solution used was rechecked.

After access was achieved, cells were allowed to stabilize for 5 min, and then alternately exposed to pH 7.3 (control) and to various more alkaline and acid pH values. To ensure complete effect in each solution with changed pH, voltage steps were made at 5 s intervals after solution change, until the effects were stable. Holding potential was −140 mV to ensure full channel availability, and cells were depolarized to potentials between −120 and +40 mV in 5 mV increments. Data were capacity corrected using 8–64 scaled summed subthreshold steps of 20 mV each, and leak corrected by the value predicted from linear fit to currents below −80 mV, or by the value interpolated between the holding current and 0 mV. Peak currents as a function of potential were fit with a Boltzmann relationship as follows:

$$I_{Na} = (V_t - V_{rev})G_{max}/(1 + \exp(V_t - V_{1/2}/k)) \quad (1)$$

where I_{Na} is the peak current in response to a step depolarization, V_t is the test potential, and the fitted parameters were: $V_{1/2}$, the half-point of the relationship; k, the slope factor (in millivolts); G_{max}, the maximum peak conductance; and V_{rev}, the reversal potential. For comparisons between cells, data were normalized to G_{max} at pH 7.3 determined before and after the intervention. The pre- and postcontrols were required to be within 10% for inclusion of the measurement in the analyses.

Normalized G_{max} (fraction G_{max}) values at various pH values were plotted and fit with a logistic function as:

$$\text{Fraction } G_{max} = A_1 + (A_2 - A_1)/1 + 10^{[(\log(pK_a) - pH)p]} \quad (2)$$

where A_1 is the pH-independent fraction, A_2 is the maximum, and pK_a is the pH at which half-maximum block occurred. Initially, p (the Hill coefficient) was allowed to vary, but all of the dose–response relationships produced fits in which p was not statistically different from unity, so p was fixed at unity for all reported data. In all titration curve analyses, each value of G_{max} measured at a pH different from 7.3 was used as an independent observation, rather than averaged with other values at that pH. The reason for this approach was that the number of observations at each pH varied, and use of averages failed to account for that in the

Table 1. Effect of vestibule mutations on pH titration of G_{max}

Channel type	n	pK_a	Acid asymptote	Alkaline asymptote	r
Nav1.4WT	47	6.3 ± 0.06	0.14 ± 0.03	1.11 ± 0.03	0.97
Nav1.4(Y401S)	31	6.3 ± 0.06	0.14 ± 0.02	1.09 ± 0.01	0.98
Nav1.4(Y401F)	20	6.3 ± 0.06	0.17 ± 0.03	1.08 ± 0.02	0.98
Nav1.4(Y401C)	26	6.1 ± 0.06	−0.02 ± 0.04	1.05 ± 0.01	0.93
Nav1.5WT	32	6.2 ± 0.08	−0.02 ± 0.04	1.05 ± 0.04	0.95
Nav1.5(C373Y)	28	6.4 ± 0.05	0.13 ± 0.02	1.10 ± 0.01	0.98

Values for pK_a, acid asymptote and alkaline asymptote are means ± S.E.M. G_{max}, maximum peak conductance.

fit. Almost all G_{max} values were from separate cells (see figure legends for numbers), because the requirement for both pre- and postcontrol measurements rarely allowed multiple measurements in one cell. Consequently, giving each relative G_{max} value equal weight in the logistic fit was statistically more accurate. Comparisons between parameters were evaluated using Student's t test, and considered significantly different when $P < 0.05$.

Data were analysed using locally written programs in Matlab (Mathworks, Natick, MA, USA) and Origin (OriginLab, Northampton, MA, USA). Results of the fitted parameters of alkaline asymptote, acid asymptote, and pK_a from the mean-least-squares fit to the logistic equation are reported in the text and Table 1 as means ± S.E.M.; r is the correlation coefficient of the mean-least-squares fit to the titration curve.

Results

pH effects on Na^+ currents and gating

Examples of currents recorded during step depolarizations at three pH values for a cell expressing $Na_V1.4$ are shown in Fig. 1. Current magnitude decreased in acid solution (Fig. 1*A*). The well-known fully reversible shift in gating that produced changes in current magnitude and time course was seen (Hille, 1968). Peak current–voltage relationships demonstrated that current size was reduced both because the voltage range over which channels activated shifted in the depolarizing direction, and because G_{max} was reduced (Fig. 1*B*). In addition, the well-documented slow time-dependent shift in gating that occurs during experiments (Hanck & Sheets, 1992) was evident in the repeated washes to pH 7.3, showing the expected larger peak currents at negative potentials, a speeding of current kinetics (not shown), but no change in G_{max}. This time-dependent shift was independent of the reversible shift in gating due to titration of external surface charges (Green *et al.* 1987; Khan *et al.* 2002). Reversal potentials in acid solutions were unchanged from those in solutions with pH 7.3, but G_{max} pH-dependently decreased in acid solution (Fig. 1*B*, inset).

Proton reductions in G_{max} were insensitive to external Na^+ concentration

To test whether protons compete with Na^+, we measured pH effects on currents in $Na_V1.4$ and $Na_V1.5$ with bath Na^+ concentrations of 140, 50, 10, 5, 2 and 1 mM. We used cell lines expressing different densities of channels, allowing a range of Na^+ concentrations to be studied under conditions where peak current magnitudes at pH 7.3 were similar, and voltage control was good. Although the isoforms studied here activated over different voltage ranges, i.e. $Na_V1.5$ activates over a 20 mV more negative voltage range than $Na_V1.4$, pH shifted gating of both isoforms and the mutants to a similar extent, and there were no systematic differences in the shifts in gating between different Na^+ concentrations (Fig. 1*C*).

The pH-dependent reductions in G_{max} were also not dependent on Na^+ concentration. Fractional reductions in G_{max} are shown in Fig. 2 for $Na_v1.4$ and for $Na_v1.5$, where each measurement in acid or alkaline solution was normalized to the bracketing value at pH 7.3. Because of the length of the protocol that requires pre- and postcontrol measurements, most relative G_{max} values are from separate cells, so each point is plotted as an independent value. Firstly, data for individual data sets by Na^+ concentration were fit to the logistic function (eqn (2)). Each data set fitted a single-site curve well, with correlation coefficients of 0.95–0.96, even with data from very low [Na^+]. However, none of the data produced statistically different values for the fitted parameters, and so the best-fit lines to the grouped data are shown. We conclude the effect of acid solution on relative current magnitude was independent of Na^+ concentration, effectively ruling out the possibility that protons and Na^+ compete as ions for some sites. Because the substitute for Na^+ in the external solution was in all cases Cs^+, these results do not rule out a non-specific monovalent cation competition with protons.

Comparison of wild-type $Na_V1.4$ and $Na_V1.5$

If the titration curves were fitted with single-site binding curves with zero asymptotes, then the calculated pK_a

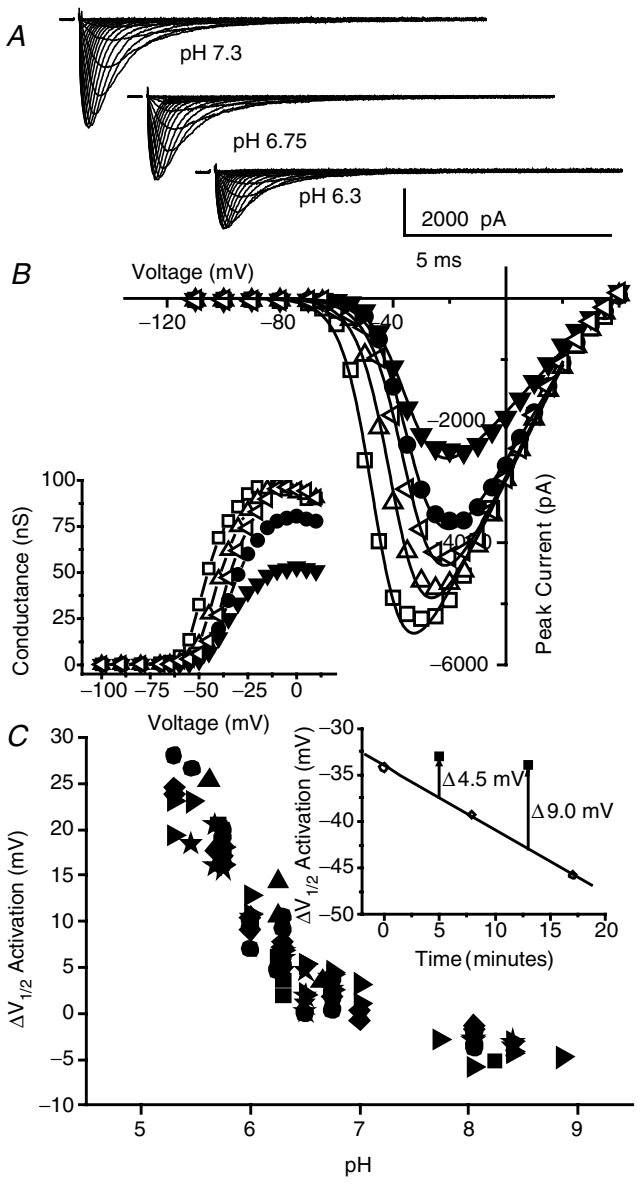

Figure 1. pH-dependent shift in kinetics
Cells were held at −140 mV and stepped to potentials between −120 and +40 mV in 5 or 10 mV increments. Peak currents were measured, plotted and fit to a Boltzmann function as described in Methods. *A*, raw currents in step depolarizations for an example cell expressing $Na_V1.4$ studied at pH 7.3, 6.75 and 6.3. Currents are shown for voltage steps beginning at −50 mV without leak correction but with capacity correction. Points between onset of the step and 0.2 ms are omitted because of incomplete capacity correction. *B*, peak current–voltage relationships from data in *A*. Data at pH 7.3 (open symbols) were obtained before and between each change in bath pH; data at pH 6.3 (▼) and pH 6.75 (●). Conductance transforms are shown in the inset. Continuous lines represent best-fit parameters for the Boltzmann fit to data between −110 and +10 mV. Fit values (±S.E.M.) for the sequentially measured current parameters are given in Table 2. There was a background hyperpolarizing shift in gating that occurred during the experiment without a change the maximum peak conductance (G_{max}). The first measurement of the half-point of the relationship ($V_{1/2}$) at pH 7.3 was −34 mV, the second was −39 mV, and the third was −46 mV. This shift was independent of the reversible depolarizing shift produced by exposure to acid solutions. Note that for this cell the combination of hyperpolarization with time, and depolarization during exposure to acid solutions, created the impression that peak currents scaled. This was coincidental (see Table 2 and Fig. 1*C* inset). *C*, protons reversibly affected the voltage range over which channels gated. Data were corrected by the amount of background shift in kinetics by linear interpolation, as illustrated in the inset for the cell illustrated in *A* and *B*. Shifts were similar for each channel isoform, and under all ionic conditions studied. The graph shows the data for the pH shift in $V_{1/2}$ of activation for $Na_V1.4$ (50 mM Na_0^+, ●, $n = 23$), $Na_V1.4$ (10 mM Na_0^+, ▲, $n = 2$), $Na_V1.4$ (140 mM Na_0^+, ■, $n = 4$), $Na_V1.5$ (50 mM Na_0^+, ⋆, $n = 19$), $Na_V1.4$(Y401C) (50 mM Na_0^+, ► $n = 22$), and $Na_V1.5$(C373Y) (50 mM Na_0^+, ◇, $n = 14$).

Table 2. Mean fit values (±S.E.M.) for the sequentially measured current parameters in Fig. 1*B*

pH	$V_{1/2}$ (mV)	k (mV)	G_{max} (nS)
7.3 (1st)	−34 ± 0.3	−6.3 ± 0.2	94 ± 2.6
6.75	−33 ± 0.3	−6.2 ± 0.2	78 ± 2.1
7.3 (2nd)	−39 ± 0.4	−5.9 ± 0.2	94 ± 2.8
6.3	−34 ± 0.5	−6.2 ± 0.3	51 ± 2.1
7.3 (3rd)	−46 ± 0.3	−5.6 ± 0.2	94 ± 2.7

$V_{1/2}$, the half-point of the relationship.

values for these two isoforms would differ (not shown). However, if the acid asymptote were allowed to be established by the best fit to the data, the pK_a values were not significantly different (both ∼6.2, Fig. 2 and Table 1), although $Na_V1.4$ had a pH-independent current of ∼14% (acid asymptote of 13.6 ± 2.9%). Surprisingly, the cardiac isoform asymptote was not significantly different from zero (−1.7 ± 3.8%). The 95% confidence limits for these asymptote values based on fitting of the entire single site curves did not overlap, implying a significant difference in their acid asymptotes. As an alternative approach to test whether these asymptotes were significantly different, fractional G_{max} values from the two isoforms made in solutions with pH 5.0 (close to the asymptote level) were compared using Student's t test ($n = 8$), which gave $P < 0.001$.

Structural basis for the pH-independent current

The amino acid composition of the predicted Na^+ channel outer vestibule is highly conserved between channel isoforms, although just above the putative selectivity filter aspartate residue $Na_v1.4$ has a tyrosine (Tyr401) and $Na_v1.5$ has a cysteine (Cys373). The amino acid at this position plays a large role in the isoform difference in guanidinium sensitivity (Backx *et al.* 1992; Heinemann *et al.* 1992; Satin *et al.* 1992; Lipkind & Fozzard, 1994). If this position also influences the pH-independent fraction, then swapping them should switch the phenotype. Figure 3 shows that the Y401C mutation of $Na_V1.4$ lost the pH-independent fraction, resulting in an acid asymptote of

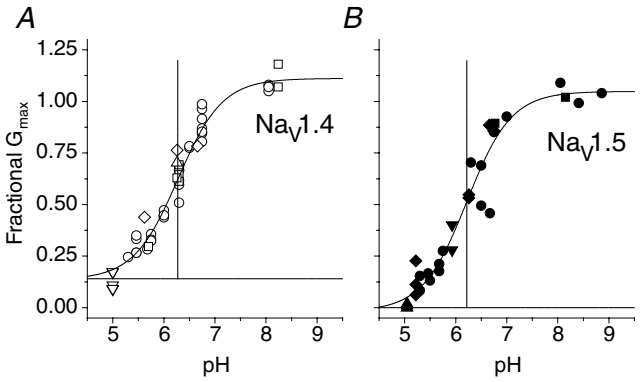

Figure 2. Titration curves of G_{max} for $Na_V1.4$ and $Na_V1.5$ in solutions of different Na^+ concentrations
For each cell, G_{max} was expressed relative to the value at pH 7.3. Continuous lines are based on best-fit values for fitted parameters to the logistic function given in Table 1. The symbols represent measurements made in different Na^+ concentrations (mM). *A*, $Na_V1.4$, 47 values derived from 39 cells. □, 140/10; ○, 50/10; ▽, 50/2; ◇, 10/10; △, 10/2. *B*, $Na_V1.5$, 32 values derived from 28 cells. ●, 50/10; ◇, 10/10; ▲, 10/2; ▼, 2/0.5; ■, 1/0.5. See text for discussion.

$-2.4 \pm 3.7\%$ (*t* test *versus* $Na_V1.4$ wild-type (WT) yielded a $P < 0.05$, $n = 12$). The mutation $Na_v1.5$(C373Y) now demonstrated an acid asymptote of $12.6 \pm 1.8\%$ (*t* test *versus* $Na_V1.5$WT yielded a $P < 0.005$, $n = 9$) (also see Table 1).

Effect of other isoform differences at this critical site

To gain insight into whether the pH-independent fraction was correlated with the presence of tyrosine or absence of cysteine at this position, we investigated other substitutions at this position. The adult brain isoform $Na_V1.2$ has a phenylalanine in this location immediately above the selectivity filter aspartate, and the peripheral nerve isoform $Na_v1.8$ has a serine in this position. $Na_V1.4$(Y401F) showed a pH-independent fraction of $17.3 \pm 2.7\%$ (*t* test *versus* $Na_V1.5$WT yielded a $P < 0.0001$, $n = 12$). $Na_V1.4$(Y401S) showed a pH-independent fraction of $12.4 \pm 2.0\%$ (*t* test *versus* $Na_V1.5$WT yielded a $P < 0.0001$, $n = 14$) (Fig. 4 and Table 1). We conclude therefore that it is not that an aromatic amino acid at this position produces the persistent current at acid pH, since a serine at this position supported current at acid pH. Rather, it is the presence of cysteine at this site that produces complete block of I_{Na} at acid pH.

Discussion

Acid solutions in a pH range that occur in human disease potently reduce voltage-gated Na^+ current. Although it has long been thought that this results from protonation of a carboxylate in the selectivity filter of the channel (Hille, 2001), we recently showed that currents are reduced in $Na_V1.4$ when the outer ring carboxylates are protonated (Khan *et al.* 2002). Although these amino acids in free solution have pK_a values in the range of 3–4, the negative field that they generate within the vestibule shifts their pK_a much more alkaline. Using our proposed model of the outer vestibule (Lipkind & Fozzard, 2000), we calculated that the selectivity filter carboxylates were protected from the effects of the negative electrostatic field because of the positive charge in the selectivity filter (lysine of the DEKA motif). Consequently, we suggested that the selectivity filter carboxylates are not protonated during acid titration. Consistent with continued function of the selectivity filter, our pH titration curve predicted a pH-independent current. Those data were obtained in oocytes, which tolerate acid solutions poorly, so that data could only be suggestive. The confirmation of a pH-independent current

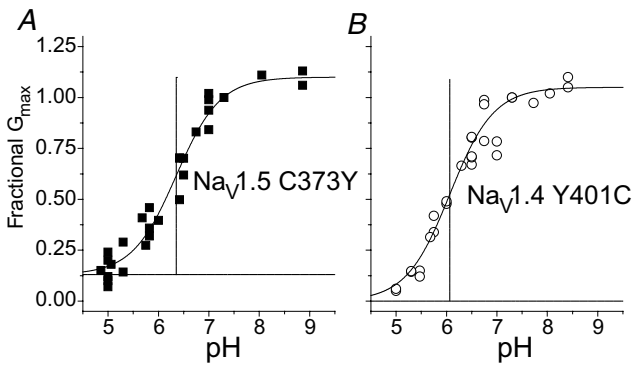

Figure 3. Titration curves for cysteine-switching mutations with asymptotes determined by fitting
For each cell G_{max} was expressed relative to the value at pH 7.3. Continuous lines are based on best-fit values for fitted parameters to the logistic function given in Table 1. *A*, $Na_V1.5$(C373Y); 28 values derived from 23 cells. *B*, $Na_V1.4$(Y401C); 26 values derived from 19 cells.

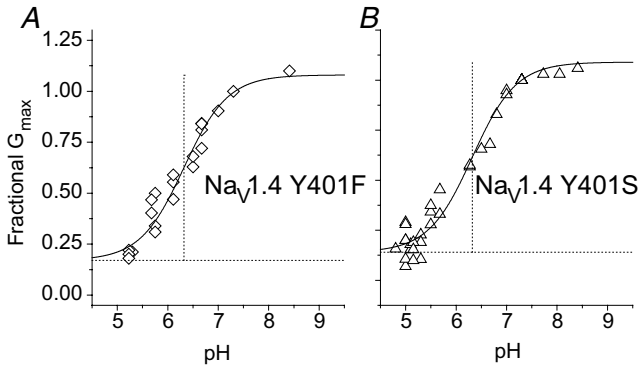

Figure 4. Titration curves for $Na_V1.4$ mutations Y401F and Y401S
For each cell, G_{max} was expressed relative to the value at pH 7.3. Continuous lines are based on best-fit values for fitted parameters to the logistic function given in Table 1. *A*, $Na_V1.4$(Y401F); 20 values derived from 20 cells. *B*, $Na_V1.4$(Y401S); 31 values derived from 31 cells.

and investigation of residues that control it were pursued here, with the goal of better understanding of the roles of carboxylates in the permeation process.

There are four experimental conclusions that we can draw from this work. First, the effects of protons on gating and reductions in current produced in acid solution are indeed independent of Na^+ concentration. Second, the titration curves are well described by a single-site relationship, but that the skeletal muscle isoform $Na_V1.4$ requires a non-zero acid asymptote – a pH-independent current of ~14% is definitely present. Third, the cardiac muscle isoform $Na_V1.5$ does not have this pH-independent current. Finally, mutational studies established that it is the presence of a cysteine in the domain I P-loop that abolishes the pH-independent current. These data all support the idea that outer ring carboxylates in the channel vestibule play a key role in permeation, and that their protonation drastically reduces permeation. Probably, the selectivity filter carboxylates remain deprotonated in acid solution because their proximity to a lysine residue (i.e. the DEKA selectivity motif) prevents the alkaline shift of their pK_a values, preserving some permeation after full protonation of the outer ring carboxylates.

Proton effects were insensitive to external Na^+ concentration

Protons can carry current through the Na^+ channel in the absence of Na^+ (Mozhayeva & Naumov, 1983), so protons might compete as cations in addition to their protonation of carboxylates. Fractional reductions in G_{max} predicted apparent pK_a values that were not different for Na^+ concentrations from 1 to 140 mM for $Na_V1.4$WT and $Na_V1.5$WT, thoroughly ruling out any significant competition. This question was previously considered in $Na_V1.4$ (Benitah *et al.* 1997). Those authors found that fractional block at Na^+ concentrations of 140, 96 and 58 mM was the same at pH 7 and 6. We did not test the possibility of non-specific competition with cations, because the ionic strength was kept constant with Cs^+ when Na^+ was lowered.

Implications of the presence of a pH-insensitive current

In all reported studies, acid titration of Na^+ current has been well represented by a single-site blocking curve. In our experiments, data for $Na_V1.4$ were also well described by a single-site titration curve, but fits required a pH-independent current of about 14%. This current may have been missed in previous experiments because few measurements below pH 6 have been reported, although one pH titration of $Na_V1.4$ (Sun *et al.* 1997) showed an acid asymptote of about 10%, similar to our measurements here.

Our interpretation that this residual current is an indication that the selectivity filter carboxylates are not protonated in acid solutions depends on two factors: effects of prior measurements of mutational neutralizations of vestibule carboxylates on single-channel conductances (Terlau *et al.* 1991; Schlief *et al.* 1996; Chiamvimonvat *et al.* 1996*a*) and results of our pH titration (Khan *et al.* 2002). The conductance effects of the mutational neutralization of outer ring carboxylates were exactly consistent with our measurements of progressive partial protonation of the outer ring carboxylates by acid solution. Our results showed that the carboxylate effects were additive, and calculation of the effect of neutralization of all four (of the outer ring carboxylates) implied a residual current of 10–15%, approximately as we found experimentally with $Na_V1.4$. On the other hand, mutational neutralization of the selectivity filter carboxylates predicts that the current would be further reduced by >95% ($6/50 \times 14/50 = 0.034$, Chiamvimonvat *et al.* 1996*a*; $0.1/15 \times 0.5/15 \approx 0$, Terlau *et al.* 1991). Therefore, the presence of a residual current implies that these selectivity filter carboxylates were not protonated, at least not by pH as low as 5.0. A further consideration is that protonation of all the vestibule carboxylates would leave a net single positive charge in the selectivity filter, which Schlief *et al.* (1996) have shown to result in a single channel conductance of $\ll$1 pS, even without change in the outer ring carboxylates. In addition, Favre *et al.* (1996) have reported that the $Na_V1.4$ selectivity ring mutation AAKA is non-functional. Finally, our calculations of electrostatic fields in the outer vestibule found that the selectivity filter lysine prevented the pK_a values of its adjacent carboxylates from shifting into the physiological range (Khan *et al.* 2002), thereby protecting them from the acid solutions.

Neutralizations of carboxylates in the selectivity filter have also been reported to change channel selectivity, e.g. neutralization of the domain II selectivity filter carboxylate Glu945 ($Na_V1.2$; Schlief *et al.* 1996) or of Glu755 ($Na_V1.4$; Favre *et al.* 1996) both changed the P_K/P_{Na} ratio. If those carboxylates had been protonated in acid solution in these experiments, then we would have expected the reversal potential to have changed. We found, however, no change in reversal potential in acid solution for any of the channels we studied. This further supports the idea that the selectivity filter carboxylates are protected from protonation during exposure to acid solution.

Lack of a pH-independent current at acid pH in the cardiac isoform was attributable to cysteine above the selectivity filter

Surprisingly, the acid asymptote for the cardiac isoform $Na_V1.5$ was not different from zero, even though the pK_a values for $Na_V1.4$ and $Na_V1.5$ were not significantly different (pK_a ~6.2). The amino acid sequences for

the P-loops thought to compose the outer vestibule are nearly identical for $Na_V1.4$ and $Na_V1.5$; specifically, the six carboxylates and the lysine are identical. Only two residues differ in the putative vestibule structure (Lipkind & Fozzard, 1994, 2000). An aspartate is found just distal to the domain I outer ring glutamate, instead of an asparagine in other isoforms, and also in domain I, the residue just external to the selectivity filter aspartate is a cysteine in $Na_V1.5$, whereas it is a tyrosine in $Na_V1.4$, a phenylalanine in the CNS isoforms, and a serine in a peripheral nerve isoform $Na_V1.8$. The aromatic residue – tyrosine or phenylalanine – appears to be responsible for the high tetrodotoxin affinities for those isoforms (Backx *et al.* 1992; Heinemann *et al.* 1992; Satin *et al.* 1992). Mutations of the tyrosine in the $Na_V1.4$ background to a phenylalanine or serine did not abolish the pH-independent conductance, although introducing a cysteine did. Likewise, introducing a tyrosine into the $Na_V1.5$ background introduced a pH-independent conductance.

It was the presence of a cysteine then rather than the absence of an aromatic residue that controlled whether conductance was present at acid pH values. Cysteine is a small sulphur-containing residue that is neutral at physiological pH, which can ionize with a pK_a of 9.0–9.5, and which shows a tendency to interact with a number of reagents. It is not plausible to postulate that deprotonation and creation of a partial negative charge is responsible for the pH-independent conductance, even though cysteine can have a shifted pK_a in enzyme active sites (Wang *et al.* 2001). Experimental introduction of a negative charge at this site in $Na_V1.5$ by reaction of the native cysteine with MTSES at physiological pH increased current slightly, rather than decreasing current magnitude (Kirsch *et al.* 1994). Cysteine has a tendency to form covalent S–S bonds, but it is also unlikely that acid solution exposed an otherwise buried cysteine, since disulphide bonds are usually stable, and the effect on Na^+ current in acid solution was immediately reversible upon return to physiological pH.

A more attractive possibility to explain the role of cysteine is that it acquires a positive charge at acid pH, either by association with a metal ion or by protonation (Creighton, 1993). Interaction of the cysteine with Cd^{2+} (Chiamvimonvat *et al.* 1996*a*), Zn^{2+} (Schild & Moczydlowski, 1994) or MTSEA/MTSET (Kirsch *et al.* 1994; Chiamvimonvat *et al.* 1996*b*) produces large reductions in current. The negative field generated by vestibule carboxylates would shift this cysteine pK in the alkaline direction, so it is plausible that in acid solution cysteine could become protonated, even though in free solution the pK_a would be predicted to be near pH 2–3. For $Na_V1.2$ and $Na_V1.4$, the bulky side chains

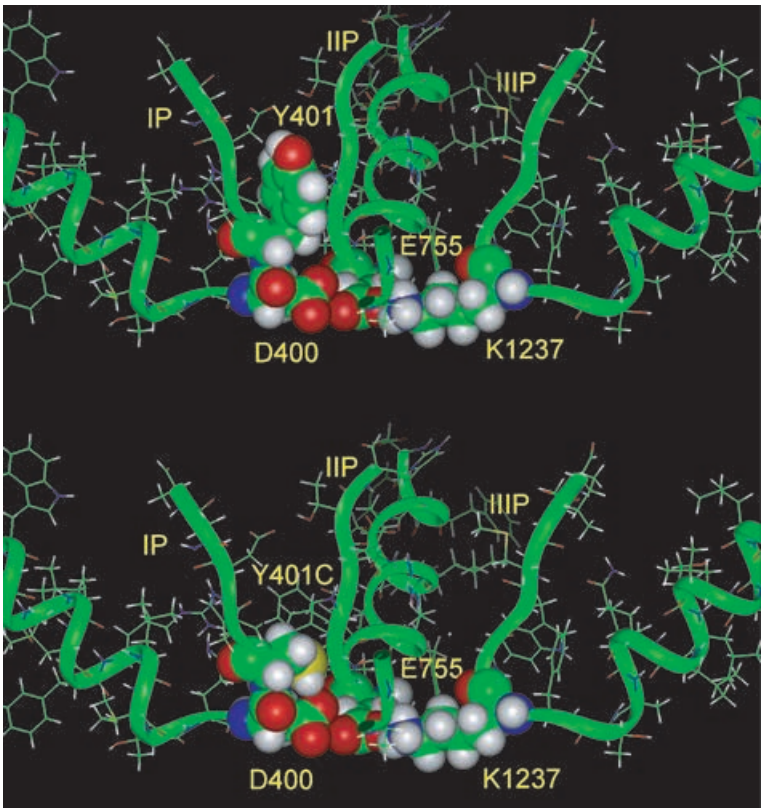

Figure 5. Model of the selectivity filter
Side-view model of the selectivity filter showing the native tyrosine in position 401 (top) and the Y401C mutant (bottom). The selectivity filter residues, and the negative tyrosine and cysteine of the Y401C, are shown as space-filled images. P loops of domains I–III are shown as green ribbons. The models were generated using the Insight and Discover graphical environment, as previously described (Lipkind & Fozzard, 1994, 2000).

of tyrosine and phenylalanine are likely to be directed away from the selectivity ring (Fig. 5*A*), because otherwise they would overlay the filter opening and occlude the pore. In contrast, the side chain of cysteine in $Na_V1.5$ is sufficiently close to the selectivity ring aspartate for hydrogen bonding, $-CH_2-SH\ldots{}^{-}OOCCH_2-$ (Fig. 5*B*). The side chain of serine is shorter and would not form a hydrogen bond. In such a configuration at very low pH (4–5), the sulfhydryl group of cysteine might be protonated. Certainly, introduction of a positive charge at this location according to the scheme $-CH_2-SH + H^+ \rightarrow -CH_2-S^+-H_2$ would block current. The pK_a of this proposed reaction under these conditions is unknown, but it would need to be in the range of pH 5 in order to minimize the acid asymptote. In the range of pH 5–6 it would not have affected the pK_a of the overall titration curve. Within the accuracy of these measurements, the pK_a of $Na_V1.5$ was not different from that of $Na_V1.4$, although the correlation coefficient r for the entire logistic fit was marginally lower (Table 1).

The P-loop carboxylates are perfectly conserved in Na^+-selective mammalian voltage-gated channels, and would be expected to generate a large negative electrostatic field (Dani, 1986; Cai & Jordan, 1990). All of the carboxylates and the cysteine are exposed to the solution, judged by their interaction with the pore-blocking guanidinium toxins (Terlau *et al.* 1991; Penzotti *et al.* 1998) and μ-conotoxin (Chang *et al.* 1998), and by cysteine mutant interaction with MTS reagents (Chiamvimonvat *et al.* 1996*a*; Tsushima *et al.* 1997). Their neutralization (by substitution with cysteine, asparagine, glutamine, or alanine) drastically reduces single-channel conductance, with Asp1241 having the least effect, Asp400 and Glu755 having the most effect (Terlau *et al.* 1991; Chiamvimonvat *et al.* 1996*b*; Favre *et al.* 1996; Schlief *et al.* 1996). The double mutant AAKA yields a non-conducting channel (Favre *et al.* 1996). The outer ring carboxylates are neutralized by protonation in acid solution (Khan *et al.* 2002), with all of them contributing to a single blocking curve, but the selectivity filter carboxylates are probably not protonated. Thus, isoforms that do not have a cysteine in the domain I P-loop, are resistant to acidosis, which is physiologically advantageous for organs such as skeletal muscle where extracellular pH can drop precipitously during exercise without loss of neuromuscular transmission (Hermansen & Osnes, 1972).

References

Backx PH, Yue DT, Lawrence JH, Marban E & Tomaselli GF (1992). Molecular localization of an ion-binding site within the pore of mammalian sodium channels. *Science* **257**, 248–251.

Benitah J, Balser JR, Marban E & Tomaselli GF (1997). Proton inhibition of sodium channels: mechanism of gating shifts and reduced conductance. *J Membr Biol* **155**, 121–131.

Cai M & Jordan PC (1990). How does vestibule surface charge affect ion conduction and toxin binding in a sodium channel? *Biophys J* **57**, 883–891.

Chang NS, French RJ, Lipkind GM, Fozzard HA & Dudley S Jr (1998). Predominant interactions between μ-conotoxin Arg-13 and the skeletal muscle Na^+ channel localized by mutant cycle analysis. *Biochemistry* **37**, 4407–4419.

Chiamvimonvat N, Perez-Garcia MT, Ranjan R, Marban E & Tomaselli GF (1996*a*). Depth asymmetries of the pore-lining segments of the Na^+ channel revealed by cysteine mutagenesis. *Neuron* **16**, 1037–1047.

Chiamvimonvat N, Perez-Garcia MT, Tomaselli GF & Marban E (1996*b*). Control of ion flux and selectivity by negatively charged residues in the outer mouth of rat sodium channels. *J Physiol* **491**, 51–59.

Creighton E (1993). *Proteins, Structures, and Molecular Properties*. Freeman, New York.

Dani JA (1986). Ion-channel entrances influence permeation. Net charge, size, shape, and binding considerations. *Biophys J* **49**, 607–618.

Favre I, Moczydlowski E & Schild L (1996). On the structural basis for ionic selectivity among Na^+, K^+, and Ca^{2+} in the voltage-gated sodium channel. *Biophys J* **71**, 3110–3125.

Green WN, Weiss LB & Andersen OS (1987). Batrachotoxin-modified sodium channels in planar lipid bilayers. Ion permeation and block. *J Gen Physiol* **89**, 841–872.

Hanck DA & Sheets MF (1992). Time-dependent changes in kinetics of Na^+ current in single canine cardiac Purkinje cells. *Am J Physiol* **262**, H1197–H1207.

Heinemann SH, Terlau H & Imoto K (1992). Molecular basis for pharmacological differences between brain and cardiac sodium channels. *Pflugers Arch* **422**, 90–92.

Hermansen L & Osnes JB (1972). Blood and muscle pH after maximal exercise in man. *J Appl Physiol* **32**, 304–308.

Hille B (1968). Charges and potentials at the nerve surface. Divalent ions and pH. *J Gen Physiol* **51**, 221–236.

Hille B (2001). *Ion Channels of Excitable Membranes*. Sinauer Associates, Sunderland, Massachusetts.

Khan A, Romantseva L, Lam A, Lipkind G & Fozzard HA (2002). Role of outer ring carboxylates of the rat skeletal muscle sodium channel pore in proton block. *J Physiol* **543**, 71–84.

Kirsch GE, Alam M & Hartmann HA (1994). Differential effects of sulfhydryl reagents on saxitoxin and tetrodotoxin block of voltage-dependent Na^+ channels. *Biophys J* **67**, 2305–2315.

Lipkind GM & Fozzard HA (1994). A structural model of the tetrodotoxin and saxitoxin binding site of the Na^+ channel. *Biophys J* **66**, 1–13.

Lipkind GM & Fozzard HA (2000). KcsA crystal structure as framework for a molecular model of the Na^+ channel pore. *Biochemistry* **39**, 8161–8170.

Mozhayeva GN & Naumov AP (1983). The permeability of sodium channels to hydrogen ions in nerve fibres. *Pflugers Arch* **396**, 163–173.

Nimigean CM, Chappie JS & Miller C (2003). Electrostatic tuning of ion conductance in potassium channels. *Biochemistry* **42**, 9263–9268.

Penzotti JL, Fozzard HA, Lipkind GM & Dudley SC Jr (1998). Differences in saxitoxin and tetrodotoxin binding revealed by mutagenesis of the Na^+ channel outer vestibule. *Biophys J* **75**, 2647–2657.

Satin J, Kyle JW, Chen M, Bell P, Cribbs LL, Fozzard HA & Rogart RB (1992). A mutant of TTX-resistant cardiac sodium channels with TTX-sensitive properties. *Science* **256**, 1202–1205.

Schild L & Moczydlowski E (1994). Permeation of Na^+ through open and Zn^{2+}-occupied conductance states of cardiac sodium channels modified by batrachotoxin: exploring ion–ion interactions in a multi-ion channel. *Biophys J* **66**, 654–666.

Schlief T, Schonherr R, Imoto K & Heinemann SH (1996). Pore properties of rat brain II sodium channels mutated in the selectivity filter domain. *Eur Biophys J* **25**, 75–91.

Sun YM, Favre I, Schild L & Moczydlowski E (1997). On the structural basis for size-selective permeation of organic cations through the voltage-gated sodium channel. Effect of alanine mutations at the DEKA locus on selectivity, inhibition by Ca^{2+} and H^+, and molecular sieving. *J Gen Physiol* **110**, 693–715.

Sunami A, Tracey A, Glaaser IW, Lipkind GM, Hanck DA & Fozzard HA (2004). Accessibility of mid-segment domain IV, S6 residues of the voltage-gated Na^+ channel to methanethiosulfonate reagents. *J Physiol* **561**, 403–413.

Terlau H, Heinemann SH, Stuhmer W, Pusch M, Conti F, Imoto K & Numa S (1991). Mapping the site of block by tetrodotoxin and saxitoxin of sodium channel II. *FEBS Lett* **293**, 93–96.

Tsushima RG, Li RA & Backx PH (1997). Altered ionic selectivity of the sodium channel revealed by cysteine mutations within the pore. *J Gen Physiol* **109**, 463–475.

Wang PF, McLeish MJ, Kneen MM, Lee G & Kenyon GL (2001). An unusually low pK_a for Cys282 in the active site of human muscle creatine kinase. *Biochemistry* **40**, 11698–11705.

Westerblad H & Allen DG (2003). Cellular mechanisms of skeletal muscle fatigue. *Adv Exp Med Biol* **538**, 563–570, and 571 (discussion).

Acknowledgements

We would like to thank J. R. Liu for his assistance in data collection, and Constance Mlecko for her creation and maintenance of stable cell lines. This work was supported by RO1 HL-65661 (H.A.F.).